


# Seismic behaviour of timber-laced stone masonry buildings before and after interventions: shaking table tests on a two-storey masonry model

Charalambos Mouzakis<sup>1</sup> · Chrissy-Elpida Adami<sup>2</sup>  ·  
Lucia Karapitta<sup>1</sup> · Elizabeth Vintzileou<sup>2</sup>

Received: 2 December 2016 / Accepted: 26 August 2017 / Published online: 21 September 2017  
© Springer Science+Business Media B.V. 2017

**Abstract** The present work focuses on the seismic behaviour of timber-laced masonry buildings with timber floors, before and after the application of intervention techniques. A two-storey building with timber ties (scale 1:2) was subjected to biaxial seismic actions. Prior to the execution of shaking table tests, the dynamic characteristics of the model were identified. The base acceleration was increased step-wise until the occurrence of significant but repairable damages. Afterwards, the masonry was strengthened by means of grouting, whereas the diaphragm action of the top floor of the building was enhanced and the model was re-tested. The tests on the timber reinforced model before strengthening show that the presence of timber ties within the masonry elements contributes to improved seismic behaviour. The performance of the model after strengthening shows that the selected intervention techniques led to a significant improvement of the seismic behaviour of the building model.

**Keywords** Timber-laced masonry · Three-leaf stone masonry · Diaphragm action · Grout injection · Seismic behaviour · Shaking table tests

---

✉ Charalambos Mouzakis  
harrismo@central.ntua.gr

✉ Chrissy-Elpida Adami  
adamis@central.ntua.gr

<sup>1</sup> Laboratory of Earthquake Engineering, Faculty of Civil Engineering, National Technical University of Athens, 9 Iroon Polytechniou str, 15773 Athens, Greece

<sup>2</sup> Laboratory of Reinforced Concrete, Faculty of Civil Engineering, National Technical University of Athens, 9 Iroon Polytechniou str, 15773 Athens, Greece

## 1 Introduction

Detailed survey of structural systems in the earthquake prone area of the Eastern Mediterranean has shown that timber laces (also called ties or reinforcement) have been used in masonry structures, in a variety of forms and arrangements, since 2500 BC (Langenbach 1989, 2002; Palyvou 1999 cited in Vintzileou 2011; Moropoulou et al. 2000; Tsakanika 2006 cited in Vintzileou 2011; Vintzileou 2008; Touliaos 2009 cited in Vintzileou 2011; Tsakanika and Mouzakis 2010; Vintzileou 2011). In numerous historic centers (more than 70 in Greece alone), constructed during the eighteenth and nineteenth centuries, timber laced masonry systems were identified and surveyed (Fig. 1). In those systems, longitudinal timber elements are placed along the perimeter of buildings at several levels (e.g. top of the foundation, floors and roof levels, around the openings, etc.). The longitudinal timber elements are connected at the corners of the buildings (Fig. 2a, b), whereas splicing is provided when the plan dimensions of the building are longer than the timber elements (Fig. 2e–h). In the most frequent case, where a pair of longitudinal timber elements are placed parallel to the faces of masonry walls, transverse timber connection of the longitudinal elements is provided at intervals (Fig. 2c, d).

The multiple beneficial effects of timber laces on the seismic behaviour of historic buildings are recognized by several researchers. For example Langenbach (2002), based on in situ observations, states that timber-laced structures have survived earthquakes thanks to their ability to dissipate seismic energy (through the straining and sliding of the joints between masonry and timber reinforcement) without undergoing significant structural degradation. However, the available literature providing quantitative data on the mechanical behaviour of timber-laced masonry structures is scarce (Touliaos 2005; Vintzileou 2008; Vintzileou and Skoura 2009). According to the results obtained by Vintzileou (2008) on timber-laced wallettes made of three-leaf stone masonry, a moderate increase of the compressive strength (by 10–20%) was recorded and attributed to the confining action of the timber laces. At the same time, the opening of vertical cracks on the faces of wallettes, as well as within the thickness of masonry was significantly reduced (by approx. 50% compared to identical unreinforced masonry wallettes). The effect of timber ties on the shear resistance of masonry was rather spectacular. The testing of timber laced wallettes under diagonal compression (Vintzileou 2008) has shown a significant increase (two to five times) of the bearing capacity of masonry, whereas masonry was able to



**Fig. 1** a, b Typical timber reinforced buildings in Greece

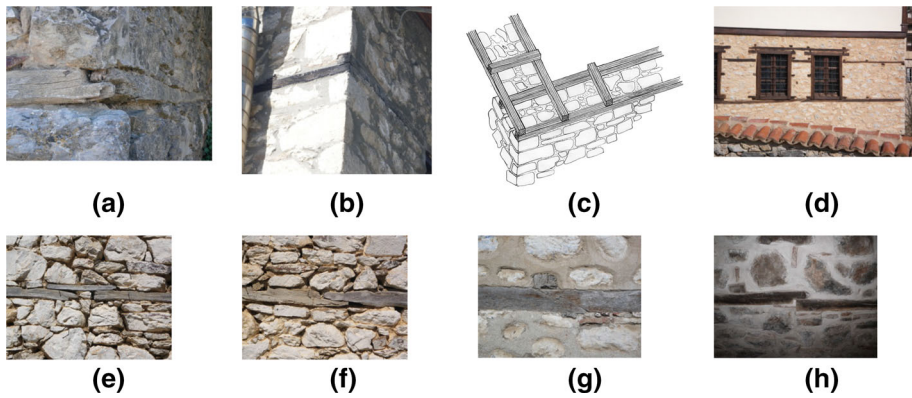


**Fig. 2** a, b Typical connections of longitudinal timber elements at the corner of the building, c sketch of longitudinal and transverse timber elements, d transverse timber elements are visible on the façade of the building, e–h alternative splices of longitudinal timber elements

undergo large deformations without being disintegrated. Similarly, preliminary analyses performed by Vintzileou and Skoura (2009) on plain and timber reinforced simple (box-type) structures subjected to seismic actions, confirmed the effect of timber ties on improving the in-plane and out-of plane response of masonry walls.

The dynamic behaviour of building models made of two- or three-leaf plain masonry was studied by several researchers (before and after the application of intervention techniques, such as grouting, stiffening of diaphragms, bracing, etc.) [see i.a. (Gavrilovic et al. 1987)-cited by Shendova et al. (2012), Tomaževic (1992), Tomaževic et al. (1993), Benedetti et al. (1998), Juhasova et al. (2008), Mazzon (2010), Meguro et al. (2012), Magenes et al. (2010, 2012a, b), Vintzileou et al. (2015)]. On the contrary, to the best of the authors' knowledge, there are no published experimental data regarding the dynamic behaviour of timber-laced masonry building models.

This paper presents the results of an experimental campaign carried out with the aim to contribute to a better understanding of the response of timber-laced masonry buildings under seismic excitations. Shaking table tests were performed on a two storey three-leaf stone masonry building model with flexible wooden floors. Timber ties were located at various levels along the height of the model. The specimen was tested before and after interventions (grouting of masonry walls and enhancement of the diaphragm action of the top floor). Thus, the positive effect of the selected intervention techniques on the seismic response of the building model was identified.

## 2 Experimental programme: timber-laced masonry building model

A two storey Timber-Laced Masonry Building Model (TLMBM) with regular in-plan geometry was constructed at a reduced scale of 1:2 (Fig. 3). The model was subjected to seismic excitations at the Laboratory for Earthquake Engineering/NTUA before and after interventions. Initially, the specimen was excited with sine sweep signals and its dynamic characteristics were determined. Seismic excitations were then applied (with gradually

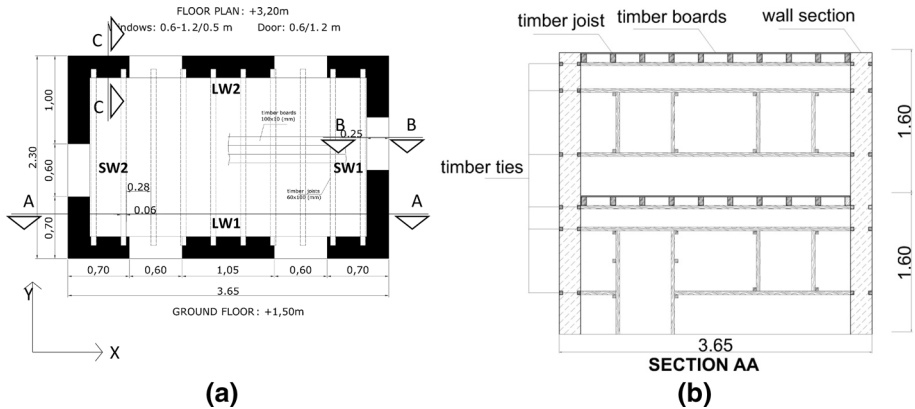


**Fig. 3** a Typical plan and b section of TLMBM

increasing acceleration) until the formation of significant, yet repairable damages. Afterwards, the damaged as-built model (TLMBM-BS) was repaired and strengthened. The applied techniques were: (a) grouting of the three-leaf masonry walls, and (b) enhancement of the diaphragm action of the top floor alone and connection of the diaphragm to the perimeter masonry (as described in Sect. 2.2.3). The stiffening of the top floor within its plane was achieved by nailing an additional timber pavement on top of the existing one, with the planks arranged at an angle of  $45^\circ$  with respect to the existing pavement. The strengthened building model (TLMBM-AS) was initially subjected to sine sweep tests and afterwards re-tested until large deformations and extensive damage occurred. Although the tested model respected the dynamic similitude laws (Harris and Sabnis 1999), the imposed seismic inputs were not time-scaled, whereas the mass simulation law could not be fully respected due to the limitations of the shaking table. More specifically, a length scale  $S_L = 1/2$  was adopted, to allow for the same materials to be used as in the prototype structure. The acceleration and the stress scales were  $S_a = 1.0$  and  $S_s = 1.0$ , respectively, both systems are subjected to gravity acceleration and the same material properties are valid for both the prototype structure and the model. According to the theory of structural models, complete dynamic similitude leads to the following scales: force scale  $S_F = 1/4$ , velocity and time scales  $S_v = S_t = 1/\sqrt{2}$ , frequency scale  $S_f = \sqrt{2}$ , density scale  $S_p = 2$ . Since the same materials were used for the construction of the model as for the prototype structure, additional masses were added to the model to respect the similitude law. Although the total mass of the model was equal to 14.5 Mgr, the additional mass was limited to 7.5 Mgr (see Sect. 2.3.1), due to the maximum capacity limitations of the shaking table. Therefore, a direct extrapolation of the results to full-scale structures may not be applied. Modeling of the scaled model and validation of the numerical model based on the experimental results is needed, before the calibrated model can be used to study the behaviour of the prototype building.

## 2.1 Geometry of TLMBM

The geometry of TLMBM is identical to that of the plain masonry specimen described in Vintzileou et al. (2015): The plan dimensions of the floor of TLMBM are  $3.65 \times 2.30$  (m<sup>2</sup>) (Fig. 3a), whereas the height of each floor is 1.60 m. The thickness of the walls is equal to 0.25 m. With the exception of a door at the ground storey, instead of a window at the first storey (Fig. 3b), the two storeys were identical. It should be noted that the geometry of the building models was dictated by several criteria, such as (a) typical characteristics of real buildings (number of storeys, almost symmetrical arrangement of openings, typical distance between consecutive bearing walls, dimensions of openings etc.) and (b) the limitations of the shaking table (in terms of maximum load, height, acceleration and displacements).

## 2.2 Materials and construction details of the experimental model

### 2.2.1 Masonry walls

The walls of TLMBM were made of three-leaf stone masonry, with leaves of approximately equal thickness. The materials used for their construction (stones, mortar, infill material, construction type of masonry and timber elements) were identical to those

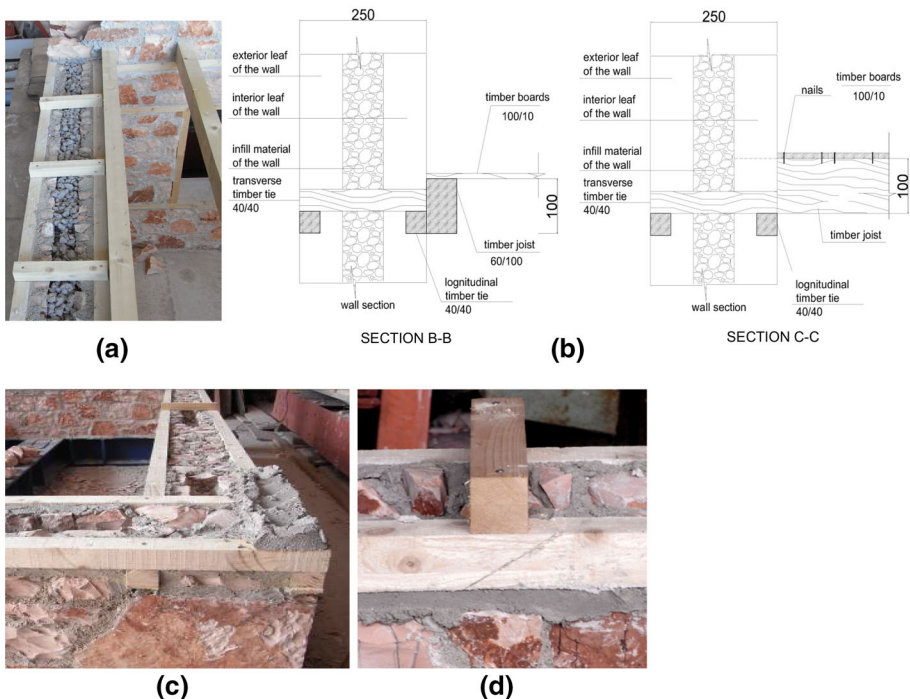


**Fig. 4** **a** In-thickness layout of longitudinal and transverse timber elements, **b** in-thickness layout of longitudinal and transverse timber elements and timber joist-to-longitudinal timber ties connection (see Fig. 3 for sections B–B and C–C), **c** connection of timber elements at the corners of the building, **d** splicing of longitudinal timber elements and connection between longitudinal and transverse elements

described in Vintzileou et al. (2015). In particular, the exterior and interior leaves of the walls were built using limestone units and a lime-pozzolan mortar. The mean compressive strength of the limestone was approximately 100 MPa, whereas the compressive strength of the mortar was approximately 4.60 MPa at the age of testing. The intermediate part of the walls was filled with pieces of stone and mortar in a proportion of 2/1 without any compaction. A system of timber laces was incorporated to the model based on the survey of historic masonry buildings in Greece. Timber ties were positioned at three levels: (a) at the bottom of openings, (b) at the top of openings and (c) at floor levels (Fig. 3b). As shown in Fig. 4a, b, two longitudinal timber elements were placed along the exterior and interior leaves of masonry (cross sectional dimensions:  $40 \times 40$  mm). Transverse timber elements (placed every 0.50 m) connected the longitudinal elements (Fig. 4a). The simplest type of connection found in historic buildings was adopted for investigation; i.e. transverse timber elements resting on and nailed to the longitudinal ones (Fig. 4a–d). Furthermore, as the longitudinal timber elements may not be available at a length equal to the length of a building, these elements need to be spliced (Fig. 4d). In this case, too, the most frequent (and least efficient) type of splicing was adopted (see also Fig. 2f): the timber elements to be spliced are cut oblique and connected with a nail. It should also be noted that the openings were provided with timber frames, connected to the timber laces (Fig. 5), as is normally the case in historic buildings (comp. Figs. 1a, 2d).

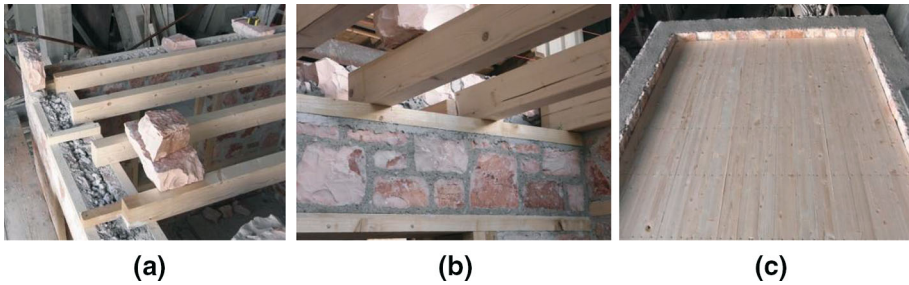
### 2.2.2 Timber floors

Figure 6 shows the typical floor construction of the TLMBM: Timber joists ( $60 \times 100$  mm<sup>2</sup>) were placed every 340 mm (Fig. 6a). The floors were resting on the masonry through the timber ties placed at the floor levels (Fig. 6a, b). As shown in Figs. 3, 4 and 6, timber joists were arranged parallel to the short walls, there was no connection between the timber floor and the short walls of the model. A timber pavement was provided, made of  $100 \times 10$  mm<sup>2</sup> boards. Each board was connected to every joist using two nails (Fig. 6c). Class C22 wood (according to EN 338) was used. Based on their geometry, the floors are classified as flexible (ASCE (2007) 41-06).



**Fig. 5** Timber ties and timber frames around openings





**Fig. 6** Structural details of the wooden floor

### 2.2.3 Repair/strengthening techniques

After the occurrence of damage, the TLMBM-BS was repaired and strengthened using the techniques described in Vintzileou et al. (2015), namely grouting of masonry and enhancement of the diaphragm action of the top floor alone.

Masonry was injected with a natural hydraulic lime based grout. The same grout was used to fill the cracks occurred to the TLMBM-BS. The mix proportions of the grout are commercial natural hydraulic lime NHL5 (90%-per weight) and a superfine natural pozzolan from Milos island, Greece (10%-per weight). The pozzolan is commercially available as  $\mu$ -silica type W. The water to solids ratio was equal to 0.825, whereas a superplasticizer (0.75%) was also added. In-situ and in-laboratory tests [i.e. stability tests, fluidity tests etc., according to Miltiadou-Fezans and Tassios (2012, 2013a, b)] were performed to characterise the grout and reach the designed properties of the grout in situ. The grout was prepared using an ultrasound mixer and injected into the masonry walls of the model (Miltiadou-Fezans et al. 2005). The total volume of the grout injected into the damaged as-built model was equal to 880lt. The percentage of voids of the filling material, calculated from grout consumption, was approximately 30%. This value is quite close to the percentage of voids in real three-leaf masonry walls.

The second technique, i.e. enhancement of the diaphragm action of the upper floor, was applied in order to enhance the box behaviour of the structure. Testing of the plain masonry model (Vintzileou et al. 2015) having shown that the model was vulnerable to out-of-plane actions mainly at the upper storey, the decision was made to explore the possibility of intervening only to the top floor, enhancing its in-plane stiffness. Such an option would be desirable, as it reduces the cost and time needed for the application of interventions, provided that its efficiency is ensured. A second timber pavement was nailed on top of the existing one: each plank of the new pavement was nailed to each timber joist using two nails. The additional planks (Fig. 7a) were laid at an angle of  $45^\circ$  with respect to the originals, based on test results obtained by Valluzzi et al. (2010). It should also be noted that the use of materials similar to the authentic ones makes the technique suitable for historic structures. The stiffened floor was connected to the perimeter walls (Fig. 7b, c). More details on the application of the second pavement and the wall-to-floor connection are given in Vintzileou et al. (2015).

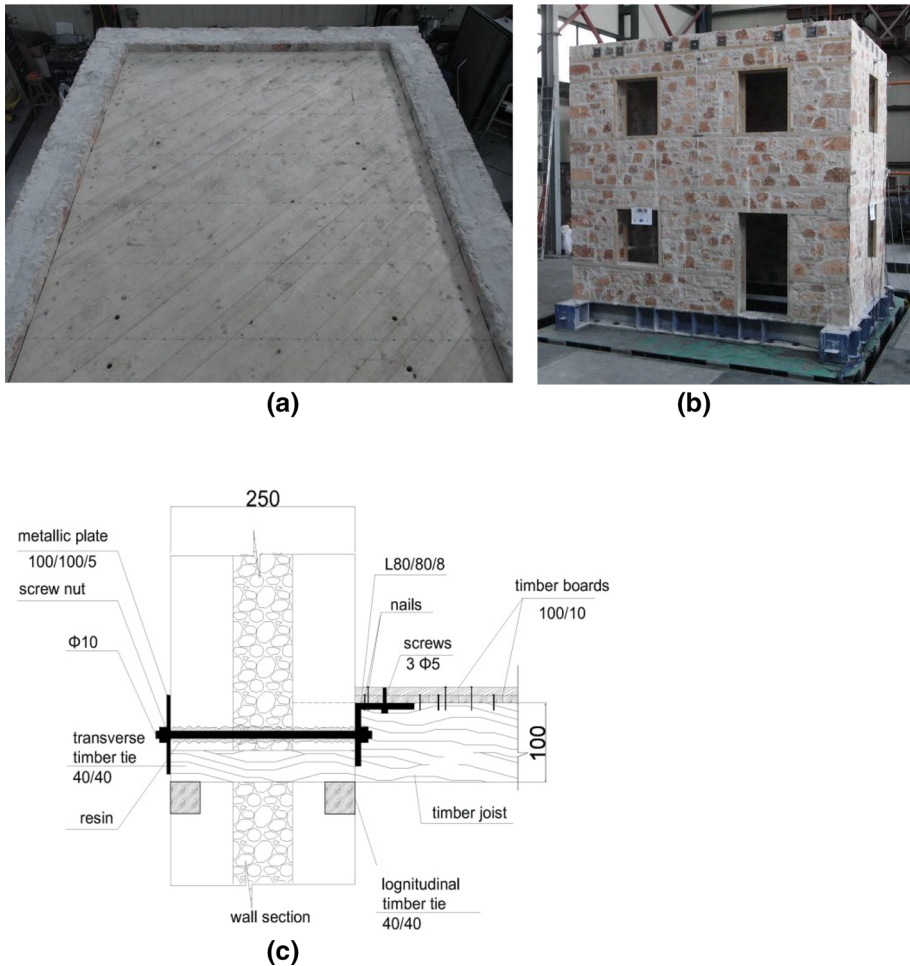


**Fig. 7** TLMBM-AS **a** top view, **b** general view and **c** wall-to-timber floor connection (detail)

## 2.3 Experimental Procedure

### 2.3.1 Test-setup and Instrumentation

The model was constructed on a stiff steel base (Fig. 7b). Deformed steel reinforcing bars were welded on the base at intervals (along two orthogonal directions) to ensure mechanical interlock between the base and the first layer of mortar and stones, preventing sliding. The steel base was securely bolted onto the shaking table.

The instrumentation of the model is shown in Fig. 8. Sixteen (16) accelerometers and twelve (12) displacement transducers were used to measure accelerations and absolute displacements along X and Y directions at floor levels.

The self-weight of the model was approximately 14.5 Mgr. Additional masses (7.5 Mgr) were placed on the two floors, namely 4.5 and 3 Mgr on the floor of the first and second storey respectively. Thus, the total mass of the as-built model was about 22 Mgr. In



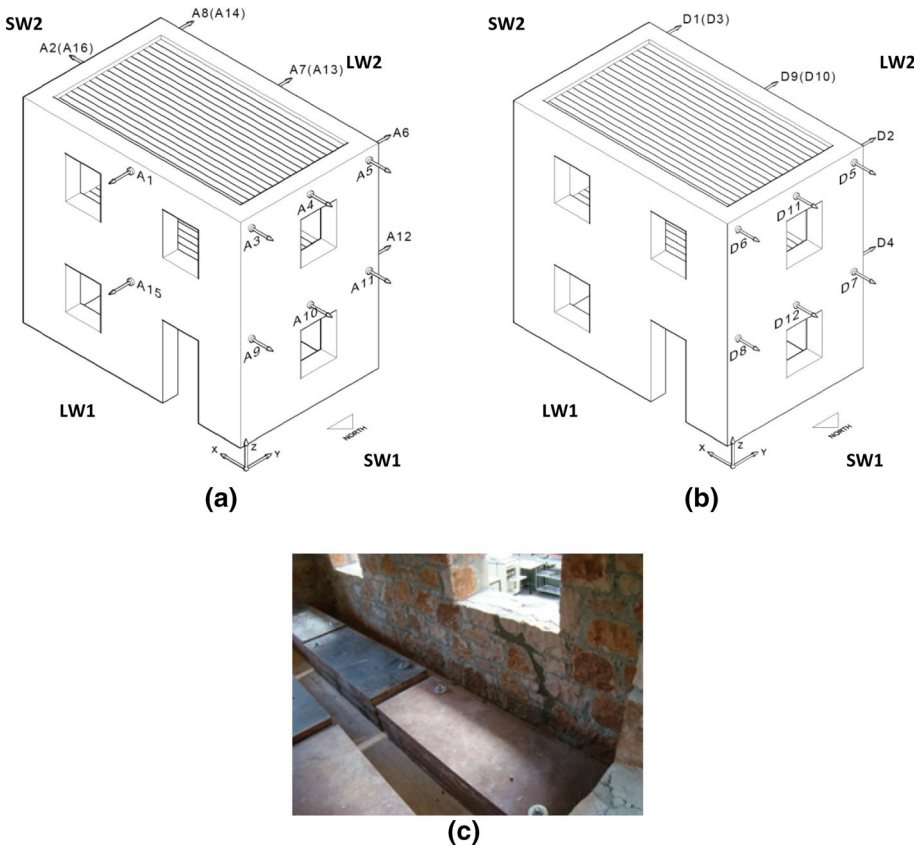


**Fig. 8** Instrumentation set-up **a** accelerometers and **b** transducers, **c** arrangement of additional masses; SW short wall and LW long wall

order to prevent any effect on the stiffness and bearing capacity of the diaphragms, each added mass was connected to the timber pavement using two 16 mm steel bolts, positioned along its diagonal (Fig. 8c). One of the two 16 mm bars was tightened, whereas the other was loose, so that each additional mass was not allowed to move either horizontally (its movement being prevented by two 16 mm bars) or vertically (its movement being prevented by one 16 mm bar). The timber joists of the floor were free to bend, as they were connected with a single 16 mm bar, to one additional mass each. After grouting, the self-weight of the model was increased by 13%, thus, the total mass of the TLMBM-AS was about 23.9 Mgr.

Since the floors were supported by the long walls of the model, the calculated compressive stress at the base of the short walls was 2% of the measured compressive strength of masonry, whereas the respective value at the base of the long walls was 7% of the compressive strength of masonry.

**Table 1** As-built model (TLMBM-BS). Test protocol

No. of test	Excitation	Direction of excitation	Base acceleration (g)/(%)	
			X	Y
1BS	Sine sweep	X	0.02	–
2BS	Sine sweep	Y	–	0.02
3BS	Kalamata	X&Y	0.045/(18%)	0.037/(14%)
4BS	Kalamata	X&Y	0.09/(36%)	0.09/(33%)
5BS	Kalamata	X&Y	0.14/(56%)	0.13/(48%)
6BS	Kalamata	X&Y	0.18/(72%)	0.18/(67%)
7BS	Kalamata	X&Y	0.22/(88%)	0.22/(81%)
8BS	Kalamata	X&Y	0.27/(108%)	0.27/(100%)
9BS	Kalamata	X&Y	0.30/(120%)	0.31/(115%)
10BS(*)	Kalamata	X&Y	0.34/(136%)	0.34/(126%)
11BS	Kalamata	X&Y	0.38/(152%)	0.33/(122%)
12BS	Sine sweep	X	0.02	–
13BS	Sine sweep	Y	–	0.02
14BS	Kalamata	X&Y	0.40/(160%)	0.38/(140%)
15BS	Kalamata	X&Y	0.44/(176%)	0.38/(140%)
16BS	Kalamata	X&Y	0.42/(168%)	0.37/(137%)

\* Occurrence of the first visible cracks

### 2.3.2 Test procedure/seismic input/test protocol

TLMBM-BS was tested on the shaking table under biaxial excitation along two horizontal axes. Before the application of the selected seismic inputs, the dynamic properties of the specimen were measured through low amplitude (0.02 g) sine logarithmic sweep excitation. Sine sweep tests were performed separately along the X and Y direction. Subsequently, the as-built model (TLMBM-BS) was subjected to a series of motions with stepwise increasing maximum base acceleration, until significant but repairable damage occurred. After the completion of the first series of tests, TLMBM was removed from the shaking table and then replaced after retrofitting. The strengthened model (TLMBM-AS) was subjected to the same series of biaxial motions until failure.

The as-built model (TLMBM-BS) was subjected to a sequence of the Kalamata earthquake [Sept. 13th, 1986, Ms = 6.2, max a = 0.25 g(X)/0.27 g(Y)]. The test protocol is given in Table 1. The accelerogram of Kalamata earthquake was selected taking into account that the major spectral amplifications of motion frequencies occur in the range of frequencies of the fundamental modes of the building model along both horizontal directions. The first cracks formed during Test 10BS. However, the input motion was further progressively increased, up to PGA values of 0.44 g (X)/0.38 g (Y), so as to cause damages of similar severity with those of the unreinforced building model (Vintzileou et al. 2015). The final Test 16BS was a repetition of Test 15BS, (Kalamata earthquake: 0.42 g(X)/0.37 g (Y), Table 1).

**Table 2** Strengthened model (TLMBM-AS). Test protocol

No. of test	Excitation	Direction of excitation	Base acceleration (g)/(%)	
			X	Y
Model TLMBM-AS1: grouting of walls				
1AS	Sine sweep	X	0.02	–
2AS	Sine sweep	Y	–	0.02
3AS	Kalamata	X&Y	0.053/(21%)	0.046/(17%)
4AS	Kalamata	X&Y	0.10/(40%)	0.097/(36%)
5AS	Kalamata	X&Y	0.15/(60%)	0.15/(56%)
6AS	Kalamata	X&Y	0.20/(80%)	0.18/(67%)
7AS	Kalamata	X&Y	0.26/(104%)	0.23/(85%)
8AS	Kalamata	X&Y	0.32/(128%)	0.25/(93%)
9AS	Kalamata	X&Y	0.34/(136%)	0.27/(100%)
10AS	Kalamata	X&Y	0.43/(172%)	0.33/(122%)
11AS	Kalamata	X&Y	0.48/(194%)	0.38 (140%)
12AS	Sine sweep	X	0.02	–
13AS	Sine sweep	Y	–	0.02
Model TLMBM-AS2: enhancement of diaphragm action of the top floor				
14AS	Sine sweep	X	0.02	–
15AS	Sine sweep	Y	–	0.02
16AS	Kalamata	X&Y	0.06/(24%)	0.06/(22%)
17AS	Kalamata	X&Y	0.10/(40%)	0.11/(41%)
18AS	Kalamata	X&Y	0.14/(56%)	0.15/(56%)
19AS	Kalamata	X&Y	0.19/(76%)	0.20/(74%)
20AS	Kalamata	X&Y	0.24/(96%)	0.23/(85%)
21AS	Kalamata	X&Y	0.30/(120%)	0.27/(100%)
22AS	Kalamata	X&Y	0.34/(136%)	0.29/(107%)
23AS	Kalamata	X&Y	0.41/(164%)	0.32/(119%)
24AS	Kalamata	X&Y	0.45/(180%)	0.35/(130%)
25AS	Sine sweep	X	0.02	–
26AS	Sine sweep	Y	–	0.02
27AS	Irpinia	X&Y	0.14(108%)	0.23/(177%)
28AS	Irpinia	X&Y	0.30/(231%)	0.39/(300%)
29AS(*)	Irpinia	X&Y	0.47/(362%)	0.72/(554%)
30AS	Irpinia	X&Y	0.66/(508%)	1.11/(854%)
31AS	Irpinia	X&Y	0.77/(592%)	1.03/(792%)

\* Occurrence of visible cracks

The same excitation sequence was adopted for the strengthened model, as well (Table 2). In order to highlight the effect of the intervention techniques on the dynamic behaviour of the structure, two distinct series of tests were performed for the TLMBM-AS, namely Phase AS-1 and AS-2. In Phase AS-1, the masonry walls were grouted and the specimen was re-tested. The strengthened model (TLMBM-AS1) reached approximately

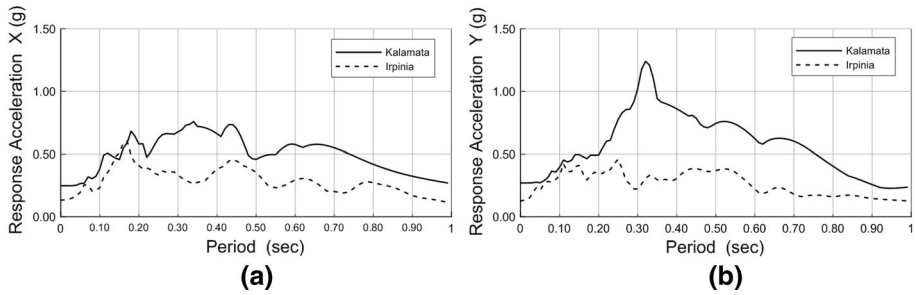


**Fig. 9** Kalamata and Irpinia earthquakes. Response spectra (5% damping) in **a** X direction and **b** Y direction

the same maximum acceleration as the as-built model [compare Test 15BS (Table 1) and Test 11AS (Table 2)], with no visible damages. Subsequently, in Phase AS-2, a second timber pavement was placed on top of the existing one at the upper level (Fig. 7a), following the same technique and arrangement as for the unreinforced masonry building model (Vintzileou et al. 2015). The strengthened model was retested, following the excitation sequence shown in Table 2. Initially, the AS-2 model was subjected to Kalamata earthquake, for base acceleration varying from 0.05 to 0.45 g. Further increase of the base motion was not possible as the allowable displacement of the shaking table (max. displacement =  $\pm 100$  mm) was exceeded. Then Irpinia earthquake was selected, taking into account that the major spectral accelerations occur at frequencies close to the fundamental frequencies of the AS-2 model and the displacement of the shaking table was not exceeded. The first part of the Irpinia earthquake signals [November 23rd, 1980, Calitri record,  $M_s = 6.9$ , max  $a = 0.13$  g(X)/0.13 g(Y)] was subsequently imposed on the strengthened model. Figure 9 shows the response spectra of the two motions for 5% damping.

### 3 Test results

In this section, the main test results (i.e. dynamic characteristics, observed damage, maximum accelerations, interstorey drifts and hysteretic response) of the building model, tested before and after interventions, are presented and commented upon.

#### 3.1 Dynamic characteristics of TLMBM-BS and TLMBM-AS building model

Sine logarithmic sweep test was performed prior to the earthquake tests, in order to determine the dynamic characteristics (natural frequencies and damping) of the model. The frequency range for the sine sweep tests was 1.0–16 Hz along X direction and 1.0–32 Hz along Y direction, at a rate of one octave per minute. Thus, the excitation frequency,  $f$  (Hz), versus time,  $t$  (s), was calculated using the expression:  $f = 1.00 \times 2^{t/60}$ .

Thus to prevent cracking of the model, a low amplitude excitation (0.02 g) was imposed. The frequencies were determined from the recorded acceleration at points A2, A3, A4, A5 for X direction and A7, A6, A8, A1 for Y direction (Fig. 8). The damping ratio was calculated using the half-power bandwidth method. The resonance frequencies and the corresponding damping ratios at measuring points of TLMBM-BS, TLMBM-AS1 and TLMBM-AS2 are shown in Fig. 10. The TLMBM-BS exhibits an average value of

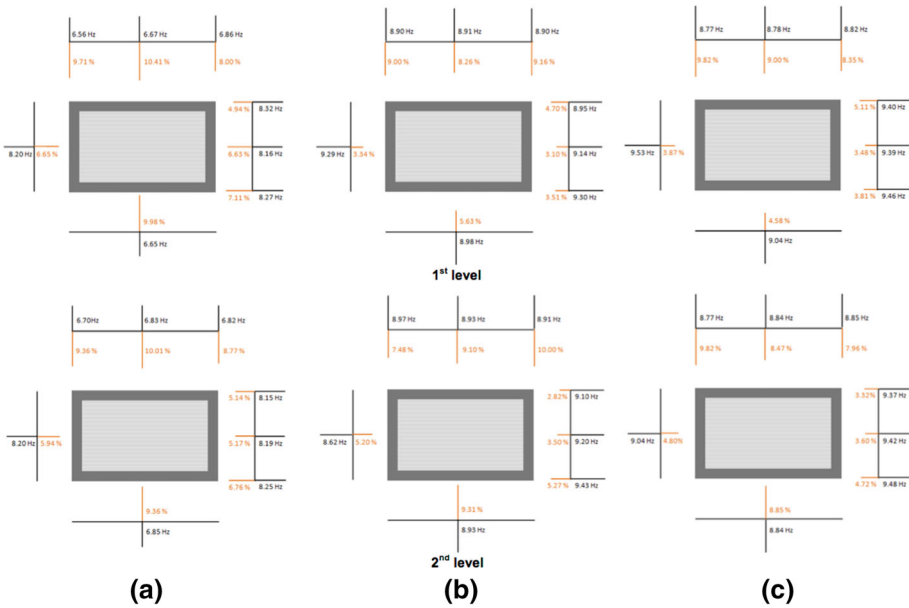


**Fig. 10** TLMBM. Resonance frequencies and damping along X and Y axes. **a** TLMBM-BS, **b** TLMBM-AS1 and **c** TLMBM-AS2

**Table 3** Model (TLMBM). Dynamic properties

Model	Frequency (Hz)		Damping (%)	
	X	Y	X	Y
TLMBM-BS before testing	8.23	6.74	5.92	9.45
TLMBM-BS after test 11BS	4.95	2.83	9.52	16.11
Model TLMBM-AS1: grouting of walls				
TLMBM-AS1 before testing	9.13	8.93	3.93	8.49
TLMBM-AS1 after Test 11AS	8.84	7.15	5.15	11.40
Model TLMBM-AS2: enhancement of diaphragm action of the top floor				
TLMBM-AS2 before testing	9.39	8.84	4.09	8.36
TLMBM-AS2 after test 24AS	7.55	7.82	7.75	8.13

frequency equal to 8.23 Hz along the X direction and 6.74 Hz along the Y direction (Table 3). The difference between these frequency values is attributed to the reduced stiffness of the building model perpendicular to its long walls. This difference is significantly reduced in TLMBM-AS1 and TLMBM-AS2; this is attributed to the improved box action of the model due to the homogenisation of masonry for TLMBM-AS1 and the stiffening of the diaphragm at the top level and improved connection to the walls for TLMBM-AS2. The damping ratio for TLMBM-BS is equal to 5.92% along the X direction (Table 3). Higher value of damping (9.45%) is measured along the Y direction, attributed



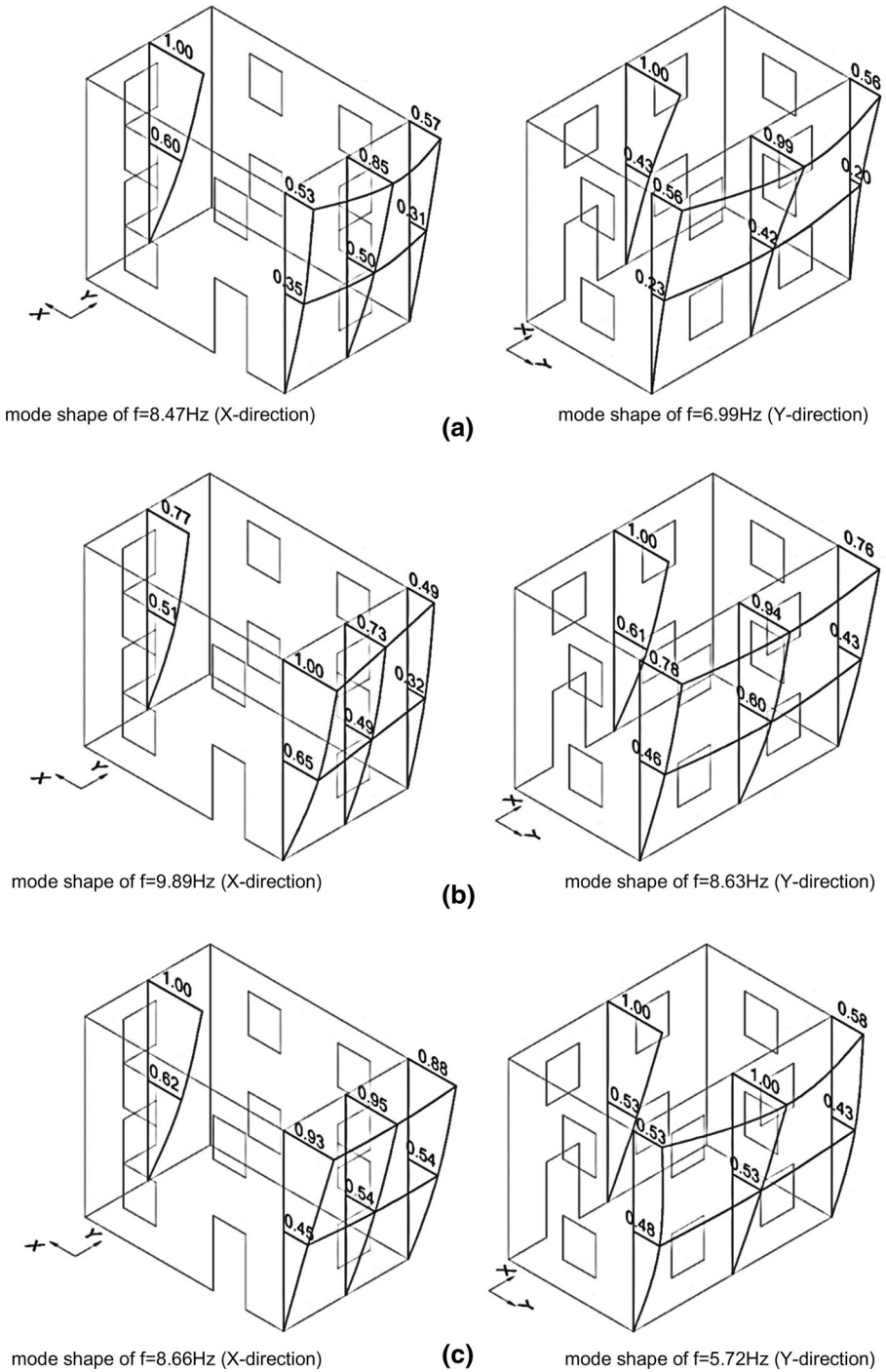


**Fig. 11** TLMBM. Normal mode shapes of the building model before and after strengthening. **a** TLMBM-BS. Test 3BS. **b** TLMBM-AS1. Test 3AS. **c** TLMBM-AS1. Test 11AS. **d** TLMBM-AS2. Test 16AS

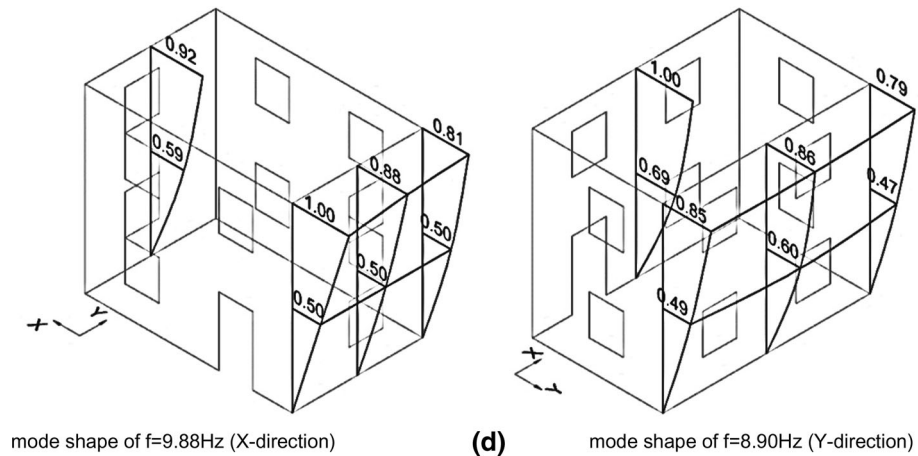


**Fig. 11** continued

to the interaction between the timber joists of the floors, as well as that of the timber ties of the walls. As expected, the occurrence of damage (Test 11BS) led to significant reduction of the frequencies for TLMBM-BS accompanied by an increase of the damping ratios. The latter might be attributed to visible, as well as to not yet visible damage, such as separation between the leaves of masonry.

Grouting of masonry led to an increase of the stiffness beyond that of the building model before testing. The increase of the frequencies for building model TLMBM-AS1 was more pronounced along the Y direction. Similarly, the damping ratio of the strengthened model TLMBM-AS1 was lower than that of the as-built model, along both directions. The first test series (Test 1AS–Test 10AS) led to a reduction of the frequencies and an increase of damping, although the model did not present any visible damage. The building model after completion of the intervention scheme, by stiffening the top floor (TLMBM-AS2) exhibited an increase of frequency. The damping ratio of the model TLMBM-AS2 was increased after the application of a series of seismic tests along both X and Y directions.

The aforementioned results are illustrated in Fig. 11, in which the modal shapes (along the X and Y directions) of TLMBM-BS (during Test 3BS), TLMBM-AS1 (during Test 3AS and 11AS) and TLMBM-AS2 (during Test 16AS) are presented. As shown in Fig. 11a, the out-of-plane deformations of TLMBM-BS recorded at mid-length of the perimeter walls are larger than those close to the corners of the building. This is due to the out-of-plane vulnerability of the walls, the in-plane flexibility of the floor diaphragms, as well as the non-monolithic behaviour of the three-leaf masonry. This is confirmed by the behaviour of the strengthened model. In the grouted model (TLMBM-AS1), the differences in deformation between mid-length and corners of the walls are reduced (comp. Fig. 11a, b). The application of a series of Kalamata earthquake to the grouted model led to the accentuation of these differences, especially along Y direction (comp. Fig. 11b, c). After stiffening of the top floor, those differences in out-of-plane deformations of walls were further reduced (comp. Fig. 11a, d), as apparently a box-type behaviour was achieved.

The variation of the equivalent elastic frequency and the equivalent damping of TLMBM-BS and TLMBM-AS throughout testing is presented in Figs. 12 and 13, respectively. These values are normalised to the values of frequency and damping ratio

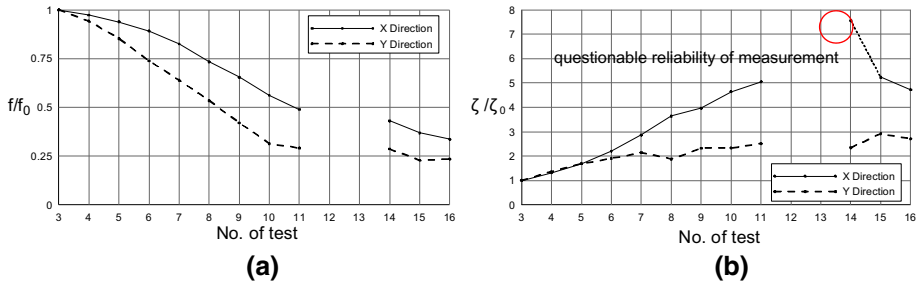


**Fig. 12** TLMBM-BS building. Values of **a** frequency and **b** damping along X and Y directions during the sequence of shaking table tests (from Test 3BS to Test 16AS, Table 1), normalised to the respective values recorded during Test3BS. Values of frequency and damping ratio measured during sine sweep tests (i.e. Tests 12BS and 13BS) are not presented

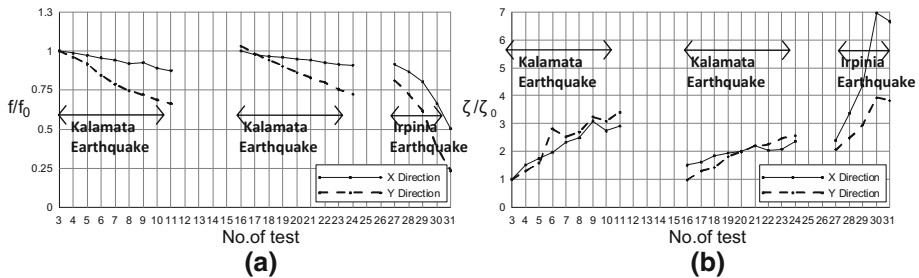


**Fig. 13** TLMBM-AS building. Values of **a** frequency and **b** damping along X and Y directions during the sequence of shaking table tests (from Test 3AS to Test 31AS, Table 2), normalised to the respective values recorded during Test3AS. Values of frequency and damping ratio measured during sine sweep tests (i.e. Tests 12AS to 15AS and Tests 25AS to 26AS) are not presented

obtained during Test 3BS and Test 3AS, respectively. Regarding the as-built model, it seems that the Kalamata earthquake has affected its behaviour along both directions. Furthermore, although the model presented visible damages during Test 10BS, a significant reduction of frequency (followed by an increase of the corresponding damping ratio) occurred much earlier (after Test 5BS, Table 1). This behaviour may be attributed to (invisible from the exterior) damage within the thickness of the three leaf walls. As expected, the grouted building model TLMBM-AS1, was mainly affected in its Y-direction by the Kalamata earthquake. Although the homogenization of masonry has reduced the vulnerability of the resulting monolithic walls to out-of-plane actions, the flexibility of the floor diaphragms is still affecting the out-of-plane behaviour (especially) of the (long) walls. Part of this vulnerability seems to persist (though for higher imposed maximum accelerations), after the stiffening of the top floor (Tests 16AS-24AS, Fig. 13a). The abrupt change of both frequency and damping during the last phase of testing is in accordance with the observed damage that became extensive during Test 29AS.

### 3.2 Observed damage

After each test, the model was carefully inspected and the observed damage was reported on drawings. Figures 14, 15 and 16 show the crack pattern of the model before and after

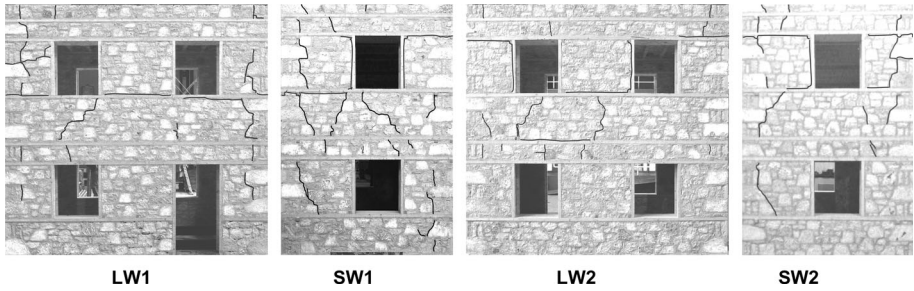


**Fig. 14** TLMBM-BS. Observed damage after Test 11BS [Kalamata earthquake: 0.38 g(X)/0.34 g(Y), Table 1]

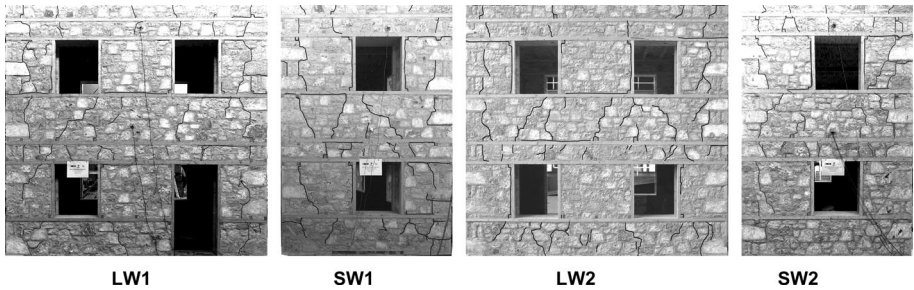


**Fig. 15** TLMBM-BS. Observed damage after Test 16BS [Kalamata earthquake: 0.42 g(X)/0.37 g(Y), Table 1]

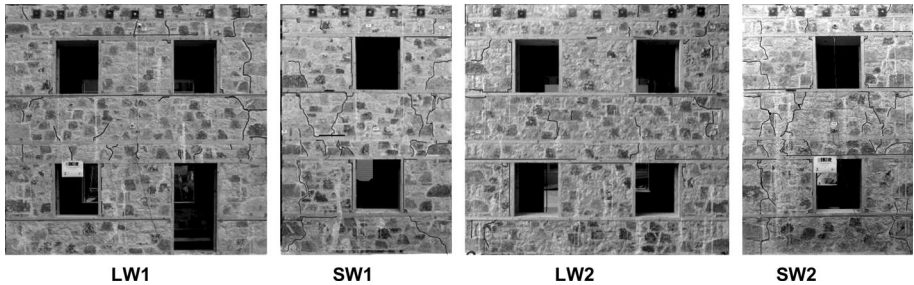


**Fig. 16** TLMBM-AS2. Observed damage after Test 31AS [Irpina earthquake: 0.77 g(X)/1.03 g(Y), Table 2]

repair and strengthening. The damages shown in Figs. 14 and 15 refer to TLMBM-BS and were surveyed after the completion of Test 11BS [Kalamata earthquake: 0.45 g(X)/0.35 g(Y)] and Test 16BS [Kalamata earthquake: 0.42 g(X)/0.37 g(Y)] respectively, whereas those presented in Fig. 16 were surveyed after the completion of Test 31AS [Irpina earthquake: 0.77 g(X)/1.03 g(Y)] for the strengthened model.

At the as-built state (TLMBM-BS), the formation of visible damages started during Test 10BS [Kalamata earthquake: 0.34 g(X)/0.34 g(Y), Table 1]. Vertical cracks and some minor shear cracks formed in the long walls after the completion of Test 11BS [Kalamata

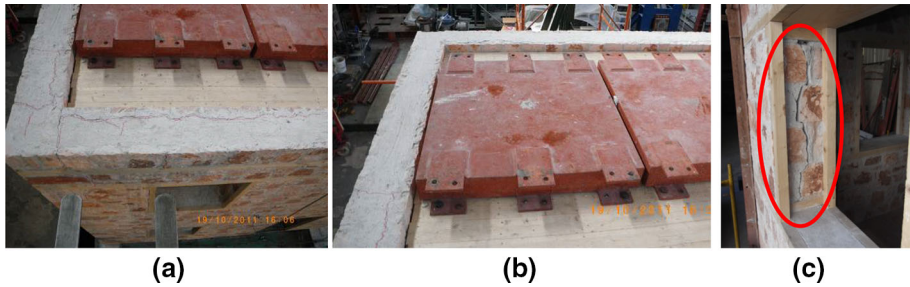


**Fig. 17** TLBMB-BS. Observed damage **a**, **b** at the roof level, **c** at the level of openings after Test 16BS [Kalamata earthquake: 0.42 g(X)/0.37 g(Y), Table 1]

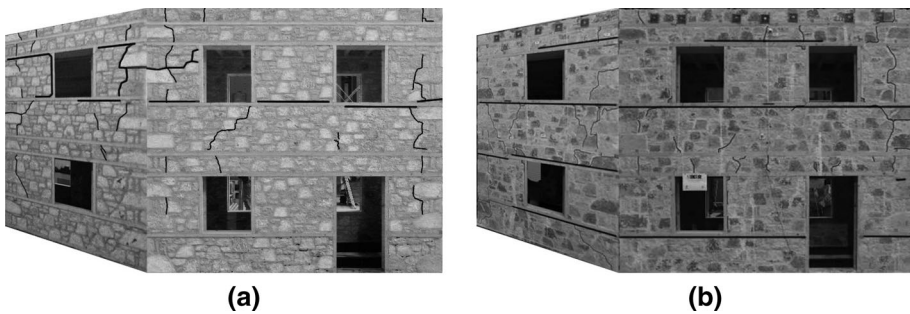


**Fig. 18** **a** TLBMB-BS specimen: rigid bodies formed during Test 11BS [Kalamata earthquake: 0.38 g(X)/0.34 g(Y), Table 1]. **b** TLBMB-AS specimen: rigid bodies formed during Test 31AS [Irpinia earthquake: 0.77 g(X)/1.03 g(Y), Table 2]

earthquake: 0.38 g(X)/0.34 g(Y), Table 1]. The width of the vertical cracks at the top was of the order of 1.0–2.5 mm, decreasing towards the base of the building. At the ground floor level only hairline cracks were visible. Although the diaphragm action of the floors was insufficient, the presence of the timber ties seems to have prevented the opening of shear cracks in the corners of doors and windows. Such cracks were limited to the short walls, having a width of the order of 1 mm. Some shear cracks also formed in the long walls. Moreover, a separation of the leaves of the three-leaf masonry was apparent (see Fig. 17a, b) after 11BS [Kalamata earthquake: 0.38 g(X)/0.34 g(Y), Table 1]. This detachment was limited to the upper part of the structure and was more pronounced along the long (from 2 to 6 mm) than along the short walls (up to 1–2 mm) of the specimen. The detachment of the leaves of masonry was visible also at the vertical sides of the windows of the upper level. It should be reminded here, that there were no header stones connecting the outer leaves of masonry. During the first test series (up to Test 11BS), it was observed that (a) cracks were of limited opening at the vicinity of timber ties (e.g. Fig. 14, observe the discontinuity of cracks at the vicinity of timber ties) and (b) separation between timber ties and masonry had occurred (Fig. 18a, observe the horizontal cracks between timber elements and masonry), mainly at the upper floor.

Moreover, further testing of the already damaged model, even by repeating the same excitation, led to generalised cracking: horizontal cracks appeared between timber ties and masonry at all levels, whereas all walls at both levels were cracked due to in-plane shear (Fig. 15). Vertical cracks between masonry and wooden frames around the openings also





**Fig. 19** TLMBM-BS. Observed damage in the walls LW2 and SW2 at the ground floor of the interior of the model after Test 16BS [Kalamata earthquake: 0.42 g(X)/0.37 g(Y), Table 1]

formed and the detachment of the leaves became more severe (Fig. 17c). Finally, Figs. 15 and 19 show similar crack pattern in the exterior and the interior faces of masonry. This is attributed to the beneficial effect of timber ties (longitudinal and transverse elements) that contribute to a more uniform distribution of vertical loads to the walls.

The strengthened model exhibited a significantly improved behaviour, in the sense that damage occurred at significantly higher maximum acceleration values than for the as-built model. Specifically, (a) TLMBM-AS1 and TLMBM-AS2 were free of visible damage after the completion of Tests 11AS and 24AS, respectively (Table 2), (b) no separation between the leaves of masonry was observed, even after the application of the strongest motion [Test 30AS, Irpinia earthquake: 0.66 g(X)/1.11 g(Y), Table 2], and (c) due to the enhanced box-action of the building, its vulnerability to out-of-plane bending was significantly reduced as vertical cracks close to the corners appeared only at an advanced stage of testing.

Moreover, the improved bond between masonry leaves (due to grouting) together with the enhancement of the diaphragm action of the top floor and its connection with the perimeter walls modified the behaviour of the building. As the seismic input increased to 300% of the Irpinia earthquake [Test 29AS, Irpinia earthquake: 0.47 g(X)/0.72 g(Y), Table 2], minor vertical cracks occurred at the corners of the building, whereas at the ground floor level, the timber ties detached from the masonry at the base of the windows. As the seismic excitation increased further, a combination of rocking of the upper floor and sliding mechanisms at the level of timber-ties was observed. At that point, significant separation occurred at the splices of the longitudinal timber elements, mainly in the short walls. With the repetition of the same seismic input [Test 31AS, Irpinia earthquake: 0.77 g(X)/1.03 g(Y), Table 2], cracking was generalised. Horizontal cracks opened at the levels of timber ties and, thus, rocking proved to be the predominant failure mechanism for TLMBM-AS (see Fig. 18b).

### 3.3 Maximum recorded accelerations

For the sequence of excitations imposed on TLMBM-BS and TLMBM-AS the recorded accelerations were increasing progressively. For the model at its as-built state, the imposed PGA has reached values up to 0.44 g (X)/0.38 g (Y) whereas for the strengthened model, reached values as high as 0.48 g(X)/0.38 g(Y) for the Kalamata earthquake and 0.66 g(X)/1.11 g(Y) for the Irpinia earthquake were reached.

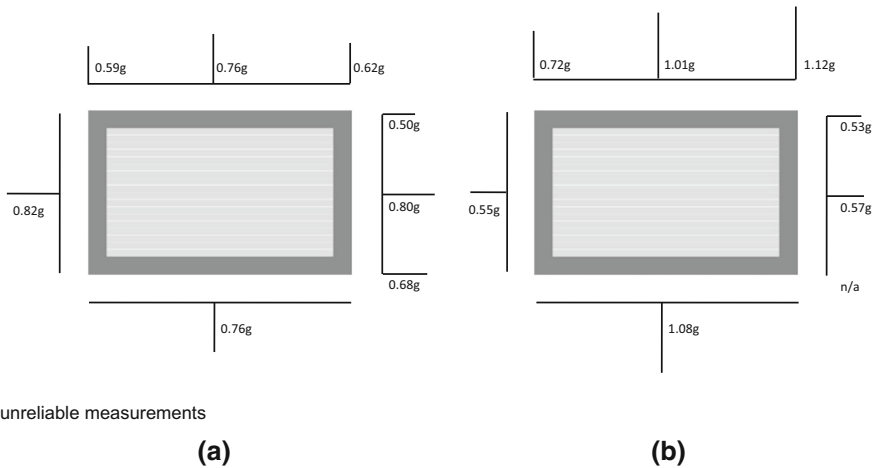


**Fig. 20** Maximum recorded accelerations **a** TLMBM-BS and **b** TLMBM-AS2

Figure 20 shows the values of the maximum accelerations recorded at the top floor in X and Y directions, for both TLMBM-BS and TLMBM-AS2. The accelerations shown in Fig. 20 were recorded during the excitations that caused damage to the model, namely Test 10BS [Kalamata earthquake: 0.34 g(X)/0.34 g(Y), Table 1] for TLMBM-BS and Test 29AS [Irpinia earthquake: 0.47 g(X)/0.72 g(Y), Table 2] for TLMBM-AS2.

For TLMBM-BS, the recorded accelerations at mid-length of both the long and short walls of the top floor are practically equal, due to the effect of interconnected timber ties. However, the accelerations measured close to the corners of the as-built model are smaller (of the order of 0.50–0.60 g) than those recorded at mid-length of the walls. This is attributed to the interconnection of walls (using large dimension stones-Fig. 7b).

In the case of the TLMBM-AS2 model, as shown in Fig. 20b, some of the accelerometers did not provide reliable measurements. However, the available measurements show similar values of acceleration at mid-length of the walls and close to the corners of the model. This is attributed to both homogenisation of masonry and stiffening of the top floor.

### 3.4 Interstorey Drift

Interstorey drift values,  $\delta$ , for both storeys of the building model were measured for Tests 10BS and 29AS (Fig. 21). Furthermore, drift values are measured for the TLMBM-AS1 specimen for the motion that corresponds to the initialisation of cracking for the TLMBM-BS specimen (Table 2: Test 10AS). The drift values reported on Fig. 21 were recorded by displacement transducers D11, D12 (X-direction) and D9, D10 (Y-direction).

The results presented in Fig. 21 allow for the following observations to be made: In TLMBM-BS, the interstorey drifts measured at mid-length of the long walls are higher than those measured at mid-length of the short walls, due to the vulnerability of the long walls to out-of-plane bending. It should be noted that the large value of interstorey drift (15.5%, Fig. 21b) is not reliable, as it is due to local damage at the location of a measuring device. Furthermore, drift values measured before and after repair and strengthening prove the efficiency of the interventions in reducing the drifts of the building model for the same

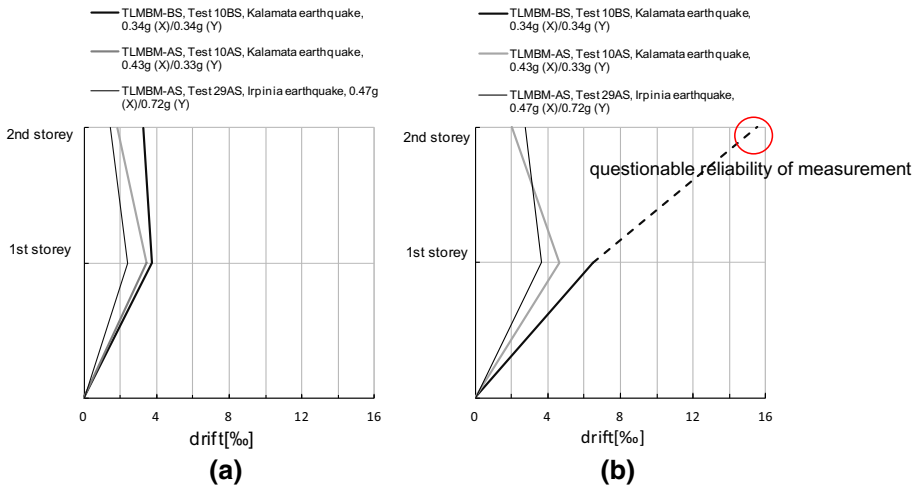


**Fig. 21** Interstorey drift values [%] along **a** X direction (along the long walls) and **b** Y direction (along the short walls) recorded for the as-built and strengthened models during Tests 10BS and 29AS

seismic input. This is more pronounced in Y-direction, i.e. perpendicular to the long walls, more vulnerable to out-of-plane actions and, expectedly, more favoured by the interventions (for example at the first level of the model: reduction varying from 8 to 54% and from 39 to 78% along X and Y direction respectively).

Drift values along Y direction measured for the strengthened model TLMBM-AS1 were lower than those obtained for TLMBM-BS. It is reminded that during Test 10BS, the as-built model was severely damaged, whereas during Test 10AS no visible damage occurred in the model TLMBM-AS1. TLMBM-AS2 was cracked under a significantly stronger excitation [in terms of maximum imposed acceleration: 0.47 g(X)/0.72 g(Y) vs. 0.34 g(X)/0.34 g(Y)] than the one that led to the formation of cracks in TLMBM-BS. The cracks of the as-built specimen were more severe and generalised than those recorded on the strengthened specimen. Moreover, for the strengthened model, the interstorey drifts at mid-length of long walls were almost equal to those at mid-length of the short walls. Therefore, the efficiency of the intervention measures in enhancing the box-action of the building model is confirmed. Finally, it should be noted that the measured  $\delta$ -values are within the limits reported in literature (Tomaževic and Weiss 2010), with drift values between 2 and 4%, measured for brick masonries (Tomaževic and Weiss 2010), as well as for three leaf masonries (Benedetti et al. 1998).

### 3.5 Hysteretic response and capacity curves

The hysteretic behaviour of the building model before and after interventions is illustrated by hysteresis loops (Figs. 22, 23, 24, 25) in terms of acceleration vs. top (relative to the base) displacement. The hysteretic curves were produced using the recorded measurements of accelerometers A4, A7 and the corresponding displacement transducers D11, D9 (Fig. 8).

The comparison of Figs. 22 and 23 shows the significantly smaller stiffness of the building model along the Y direction, as well as the larger displacements along its weak Y

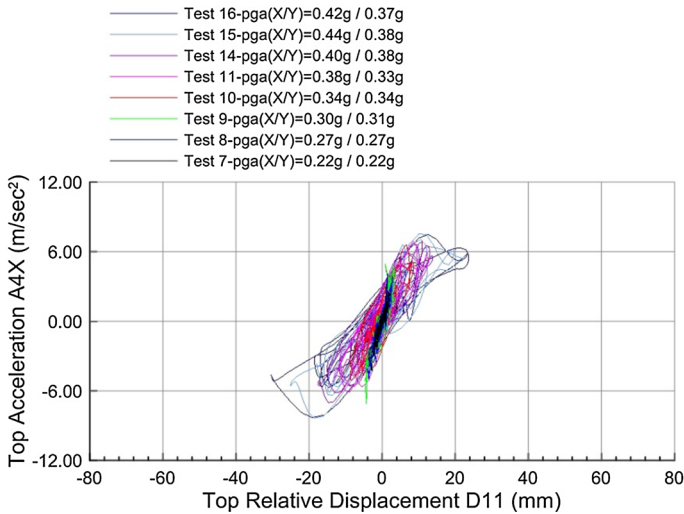


**Fig. 22** TLMBM-BS. Absolute acceleration versus top relative displacement along X direction for Kalamata base motion

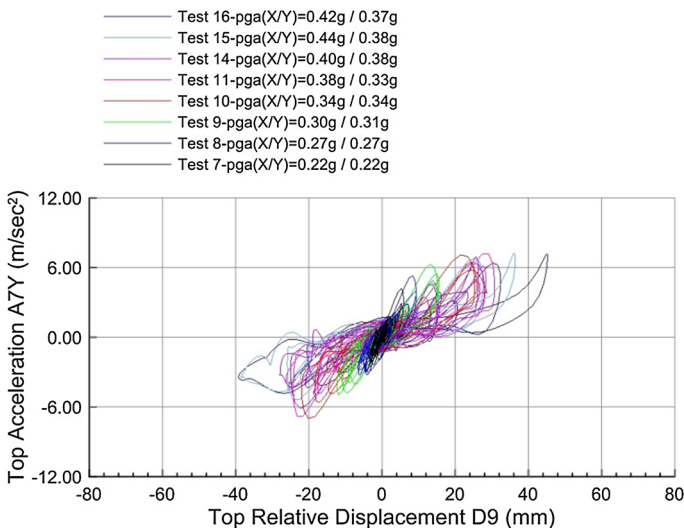


**Fig. 23** TLMBM-BS. Absolute acceleration versus top relative displacement along Y direction for Kalamata base motion

direction. As expected, the occurrence of damage causes a gradual decrease of stiffness in both directions.

Comparing Figs. 24 and 25, it is evident that the behaviour of the model after strengthening is very similar in both directions. This is not true for the last two tests, where the rocking-sliding mechanism appeared.

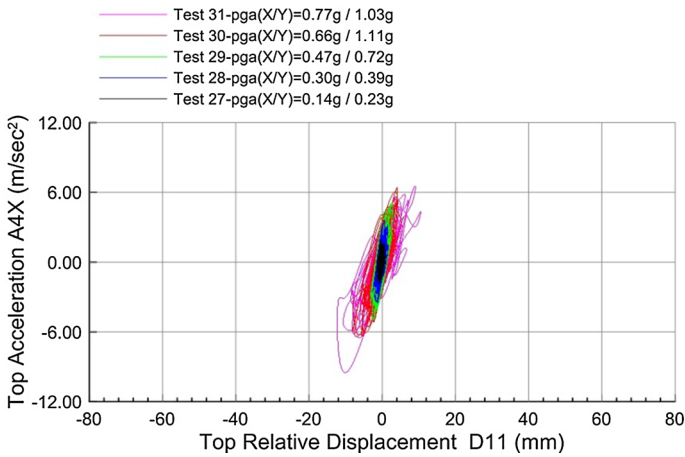


**Fig. 24** TLMBM-AS2. Absolute acceleration versus top relative displacement along X direction for Irpinia base motion

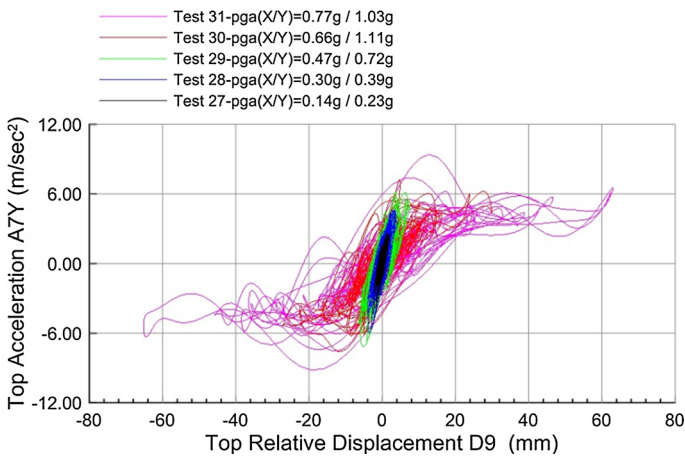


**Fig. 25** TLMBM-AS2. Absolute acceleration versus top relative displacement along Y direction for Irpinia base motion

The hysteresis loops of Figs. 22, 23, 24 and 25 demonstrate the positive effect of the applied interventions, in terms of maximum sustained acceleration, as well as in terms of deformations sustained by the building model.

Capacity curves of the tested models were derived as envelopes of the hysteretic loops. The base force was calculated as the sum of inertia forces (the product of the effective mass and the corresponding acceleration) at each floor level. The signals recorded by the displacement transducers at the mid-length of the top floor were used as relative displacement values in X and Y direction. The capacity curves for TLMBM before and after strengthening are presented in Fig. 26, while some key test results are summarised in Table 4.



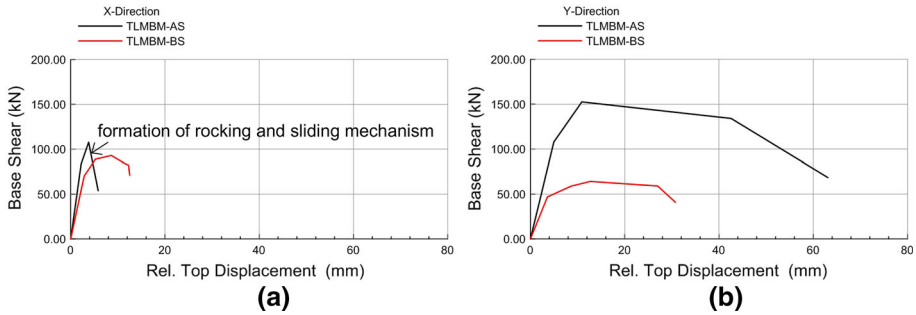


**Fig. 26** TLMBM: Capacity curves before and after strengthening in **a** X-direction and **b** Y-direction

**Table 4** TLMBM. Elastic stiffness, base shear and top displacement obtained by the envelope curves

Model	X-direction			Y-direction		
	Elastic stiffness (kN/m)	Base shear (kN)	Displacement at 80% of load (on the falling branch) (mm)	Elastic stiffness (kN/m)	Base shear (kN)	Displacement at 80% of load (on the falling branch) (mm)
TLMBM-BS	24,526.52	92.92	12.45	12,991.69	64.16	28.59
TLMBM-AS2	37,662.16	107.67	4.61	21,714.29	152.51	46.32

The comparison of the capacity curves before and after intervention, as well as the data of Table 4 show that the elastic stiffness of the strengthened building model was significantly increased (by more than 50%) in both X and Y directions. An increase in the force-response was also recorded (by 15 and 130% along X and Y direction respectively). This increase in base shear was much higher perpendicularly to the long walls and it is attributed to the beneficial effect of both grouting and enhancing the diaphragm action of the top floor. After strengthening, the behaviour perpendicular to the short walls remains practically elastic for the entire series of seismic tests. During the last seismic test, corresponding to large acceleration values, appearance of the rocking-sliding mechanism led to a pronounced reduction of base shear. It should be noted that an equally high force-response degradation was recorded during the last seismic test perpendicularly to the long walls, as well. However, in this case, an increase of the ductility of the order of 60% was recorded after strengthening. Finally, the building model, after strengthening, was able to undergo high acceleration values with extensive damage, but without collapse.

## 4 Conclusions

The shaking table tests on a timber-laced three-leaf stone masonry building model, before and after strengthening, allow for the following conclusions to be drawn:

1. The building model was provided with rather flexible in its plane diaphragms at floor levels. As a result, during testing at the as-built state, cracks formed due to out-of-

plane bending of the long walls and detachment occurred between the leaves of masonry. However, this detachment was limited due to the positive effect provided by the timber laces (at intervals along the height of the model) on the transverse connection between the masonry leaves.

2. The repetition of the same input motion to the already damaged model resulted to significant structural degradation of the building. Therefore, it can be suggested that immediate repair and strengthening measures need to be taken, after the occurrence of a seismic event, to prevent collapse and provide sufficient protection of the built cultural heritage.
3. After strengthening, the building model could withstand significantly stronger input motions. Due to the enhanced box action provided by the intervention techniques, the vulnerability of the model to out-of-plane actions was efficiently reduced. Thus, the predominant failure mode was characterized by in-plane shear of the walls, whereas rocking was observed at the locations of timber ties. It was observed that timber laces predetermine the location of horizontal cracks, while they are efficient in preventing the occurrence of in-plane cracks of masonry elements or in limiting their opening. Timber ties provided a rather uniform distribution of vertical loads to the walls, thus limiting the eccentricity due to the fact that the timber beams of floors transfer loads mainly to the interior leaf of masonry. This is confirmed by the similarity of the crack pattern surveyed on the exterior and the interior face of masonry walls.
4. Grouting of masonry led to an increase of stiffness and mass, while simultaneously reducing damping ratio. Stronger input motions, applied subsequently to the model, led to an increase of the damping. Nevertheless, neither visible damage of masonry nor decrease of the overall stiffness was recorded. Such a behaviour may be attributed to internal micro-cracking of masonry, as well as to friction between masonry and timber ties.
5. Grouting prevented the detachment of masonry leaves, thus ensuring an improved behaviour of the model against both in-plane and out-of-plane actions. Moreover, the enhancement of the in-plane stiffness of the upper-level floor, along with the efficient connection between the floor and the perimeter walls, have improved the box action of the model, enhancing its global stiffness and bearing capacity and reducing deformations and interstorey drifts, even for strong input motions. Enhancing the diaphragm action of the top floor alone proved to be beneficiary in this case. This finding, which needs to be further investigated, might offer a promising solution for interventions to historic buildings, as it reduces intervention costs and avoids suspension of the use of the entire building.
6. In general, the experimental results presented in this paper prove the efficiency of the system of timber-laced masonry, adopted in numerous earthquake prone areas, in resisting seismic actions. Furthermore, rather simple intervention techniques, compatible with the values of historic structures, were shown to improve the seismic behaviour of the building model.
7. Finally, it should be reminded that the building model was subjected to numerous seismic tests. Therefore, the behaviour exhibited at each seismic test (after the occurrence of damage) is negatively affected by the loading history. However, even under such adverse conditions, the building model was able to withstand strong motions with generalized damage, yet without collapse.

**Acknowledgements** This research was carried out within the FP7 funded European Programme NIKER (Project Contract No. 244123), <http://www.niker.eu/>.

## References

- ASCE (2007) 41-06 Seismic rehabilitation of existing buildings. ASCE/SEI 41-06, American Society of Civil Engineers, Reston, Virginia
- Benedetti D, Carydis P, Pezzoli P (1998) Shaking table tests on 24 simple masonry buildings. *Earthq Eng Struct Dyn* 27(1):67–90
- Gavrilovic P, Stankovic V, Bojadziew M (1987) Experimental investigation of a model of masonry building on seismic shaking table. In: VIII congress of structural engineers, YU
- Harris H, Sabnis G (1999) Structural modeling and experimental techniques, 2nd edn. CRC Press
- Juhasova E, Sofronieb R, Bairrao R (2008) Stone masonry in historical buildings—ways to increase their resistance and durability. *Eng Struct* 30:2194–2205
- Langenbach R (1989) Bricks, mortar, and earthquakes, historic preservation vs. earthquake safety. *APT Bull* 213(3/4):30–43
- Langenbach R (2002) Survivors among the ruins: traditional houses in earthquakes in Turkey and India. *APT Bull* 33(2/3):47–56
- Magenes G, Penna A, Galasco A (2010) A full-scale shaking table test on a two-storey stone masonry building. In: Proceedings of the 14th European conference on earthquake engineering, Ohrid, August 30–September 3 2010
- Magenes G, Penna A, Rota M, Galasco A, Senaldi I (2012a) Shaking table test of a full scale stone masonry building strengthened maintaining flexible floor and roof diaphragms. In: Proceedings of the 8th international conference on structural analysis of historical construction, Wroclaw, Poland
- Magenes G, Penna A, Rota M, Galasco A, Senaldi I (2012b) Shaking table test of a full scale stone masonry building with stiffened floor and roof diaphragms. In: Proceedings of the 15th world conference on earthquake engineering, 24–28 September 2012, Lisbon, Portugal
- Mazzon N (2010) Influence of grout injection on the dynamic behaviour of stone masonry buildings. PhD Thesis, University of Padova
- Meguro K, Navaratnaraj S, Sakurai K, Numada M (2012) Shaking table tests on ¼ scaled shapeless stone masonry houses with and without retrofit by polypropylene band meshes. In: Proceedings of the 15th world conference on earthquake engineering, 24–28 September 2012, Lisbon, Portugal
- Miltiadou-Fezans A, Tassios TP (2012) Fluidity of hydraulic grouts for masonry strengthening. *Mater Struct* 45(12):1817–1828
- Miltiadou-Fezans A, Tassios TP (2013a) Stability of hydraulic grouts for masonry strengthening. *Mater Struct* 46(10):1631–1652
- Miltiadou-Fezans A, Tassios TP (2013b) Penetrability of hydraulic grouts. *Mater Struct* 46(10):1653–1671
- Miltiadou-Fezans A, Papakonstantinou E, Zambas K, Panou A, Frantzikinaki K (2005) Design and application of hydraulic grouts of high injectability for structural restoration of the column drums of the Parthenon Opisthodomos. In: International conference on structural studies, repairs and maintenance of architectural heritage IX, 2005
- Moropoulou A, Cakmak AS, Lohvync N (2000) Earthquake resistant construction techniques and materials on Byzantine monuments in Kiev. *Soil Dyn Earthq Eng* 19(8):603–615
- Palyvou C (1999) Akrotiri-Thera: the art of construction. Library of the Archaeological Society of Athens, No 183 (in Greek)
- Shendova V, Rakicevic Z, Krstevska L, Tashkov L, Gavrilovic P (2012) Shaking table testing of models of historic buildings and monuments—IZIIS' experience, role of seismic testing facilities in performance-based earthquake engineering geotechnical. *Geol Earthq Eng* 22:221–245
- Tomaževic M (1992) Seismic rehabilitation of existing masonry buildings: research and practical implications. In: International symposium on earthquake disaster prevention, Mexico, 18–21 May 1992, vol 2, pp 260–276
- Tomaževic M, Weiss P (2010) Displacement capacity of masonry buildings as a basis for the assessment of behavior factor: an experimental study. *Bull Earthq Eng* 8(6):1267–1294
- Tomaževic M, Lutman M, Velechovsky T (1993) Aseismic strengthening of old stone-masonry buildings: is the replacement of wooden floors with R.C. slabs always necessary? *Eur Earthq Eng* 2:34–46
- Touliatos P (2005) The box framed entity and function of the structures: the importance of wood's role. In: Conservation of historic wooden structures: proceedings of the international conference, Florence, 22–27 February 2005

- Touliatos P (2009) The Doheiarion Monastery in Mount Athos—The Architecture of the Katholikon and the Tower, National Technical University of Athens, 2009, 134 pp (**in Greek**)
- Tsakanika E (2006) The structural role of timber in the masonry of palace type buildings in the Minoan Crete, Ph.D. thesis, Faculty of Architecture, National Technical University of Athens (**in Greek**)
- Tsakanika E, Mouzakis H (2010) A post-byzantine mansion in Athens. The restoration project of the timber structural elements. In: Proceedings of the world conference on timber engineering
- Valluzzi M-R, Garbin E, Dalla Benetta M, Modena C (2010) In-plane strengthening of timber floors for the seismic improvement of masonry building. World Conference of Timber Engineering, Italy
- Vintzileou E (2008) Effect of timber ties on the behaviour of historic masonry. *J Struct Eng* 134(6):961–972
- Vintzileou E (2011) Timber-reinforced structures in Greece: 2500 BC–1900 AD. *Proc Inst Civil Eng Struct Build* 164(SB3):167–180
- Vintzileou E, Skoura A (2009) Seismic behaviour of timber reinforced masonry buildings. In: Proceedings of the 1st international conference on protection of historical buildings, PROHITECH, Rome, in electronic form
- Vintzileou E, Mouzakis Ch, Adami C-E, Karapitta L (2015) Seismic behavior of three-leaf stone masonry buildings before and after interventions: shaking table tests on a two-storey masonry model. *Bull Earthq Eng* 13(10):3107–3133